DXA-based statistical models of shape and intensity outperform aBMD hip fracture prediction: A retrospective study

Bone 182 (2024) 117051

Contents lists available at ScienceDirect

Bone

journal homepage: www.elsevier.com/locate/bone

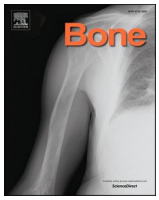

Full Length Article

DXA-based statistical models of shape and intensity outperform aBMD hip fracture prediction: A retrospective study

Alessandra Aldieri [a,b,*], Margaret Paggiosi [c,d], Richard Eastell [d], Cristina Bignardi [a,b], Alberto L. Audenino [a,b], Pinaki Bhattacharya [c,e], Mara Terzini [a,b]

[a] Polito[BIO]MedLab, Politecnico di Torino, Italy
[b] Department of Mechanical and Aerospace Engineering, Politecnico di Torino, Torino, Italy
[c] INSIGNEO Institute for In Silico Medicine, University of Sheffield, Sheffield, UK
[d] Faculty of Health, Division of Clinical Medicine, School of Medicine and Population Health, University of Sheffield, UK
[e] Department of Mechanical Engineering, University of Sheffield, Sheffield, UK

ARTICLE INFO

Keywords:
Hip fracture
Fracture prediction
Partial least square
Statistical shape-intensity model
DXA images

ABSTRACT

Areal bone mineral density (aBMD) currently represents the clinical gold standard for hip fracture risk assessment. Nevertheless, it is characterised by a limited prediction accuracy, as about half of the people experiencing a fracture are not classified as at being at risk by aBMD. In the context of a progressively ageing population, the identification of accurate predictive tools would be pivotal to implement preventive actions. In this study, DXA-based statistical models of the proximal femur shape, intensity (i.e., density) and their combination were developed and employed to predict hip fracture on a retrospective cohort of post-menopausal women. Proximal femur shape and pixel-by-pixel aBMD values were extracted from DXA images and partial least square (PLS) algorithm adopted to extract corresponding modes and components. Subsequently, logistic regression models were built employing the first three shape, intensity and shape-intensity PLS components, and their ability to predict hip fracture tested according to a 10-fold cross-validation procedure. The area under the ROC curves (AUC) for the shape, intensity, and shape-intensity-based predictive models were 0.59 (95%CI 0.47–0.69), 0.80 (95%CI 0.70–0.90) and 0.83 (95%CI 0.73–0.90), with the first being significantly lower than the latter two. aBMD yielded an AUC of 0.72 (95%CI 0.59–0.82), found to be significantly lower than the shape-intensity-based predictive model. In conclusion, a methodology to assess hip fracture risk uniquely based on the clinically available imaging technique, DXA, is proposed. Our study results show that hip fracture risk prediction could be enhanced by taking advantage of the full set of information DXA contains.

1. Introduction

Hip fractures represent the most compelling burden of osteoporosis on health care systems and expenditure [1]. The exponential increase of hip fractures with ageing is associated with a decrease in bone mass and deterioration of bone microstructure due to osteoporosis, along with additional non-skeletal factors such as an increased propensity to fall. Currently, areal bone mineral density (aBMD), measured using dual energy X-ray absorptiometry (DXA) represents the clinical gold standard for assessing hip fracture risk. By comparing the aBMD value of a subject to the aBMD of a reference young and healthy population in terms of standard deviations, the T-score is obtained, which is employed to classify the subjects as healthy, osteopenic, osteoporotic [2]. Nevertheless, there has been growing evidence concerning the limitations of T-score and other clinical indicators such as FRAX or Garvan in accurately predicting hip fracture risk [3,4]. Early diagnosis of increased hip fracture risk and consequent prophylactic treatment are the real prevention tools with which to limit bone deterioration and the consequential loss in functionality for patients experiencing fractures [5].

During the last few decades, several research groups have worked on the identification of alternative approaches to enhancing hip fracture risk prediction. Bio-mechanistic three-dimensional models, based on quantitative computed tomography (QCT) images, have been developed and demonstrated good accuracy for hip fracture prediction [6–13]. In spite of this, the latest positions statement issued by the International Society of Clinical Densitometry (ISCD) in 2019 stated that QCT-based

* Corresponding author at: Polito[BIO]MedLab, Politecnico di Torino, cso Duca degli Abruzzi 24, Torino 10129, Italy.
E-mail address: alessandra.aldieri@polito.it (A. Aldieri).

https://doi.org/10.1016/j.bone.2024.117051
Received 13 December 2023; Received in revised form 13 February 2024; Accepted 15 February 2024
Available online 20 February 2024

finite element (FE) models are to be considered comparable to aBMD in their ability to predict hip fractures [14]. Generally, the clinical adoption of these FE-based approaches has been slow. This may be due, primarily, to the lack of available large clinical validation studies reporting a statistically significant improvement in their ability to predict hip fracture over aBMD alone. In addition to this, the higher radiation exposure and cost of QCT compared to DXA scans, the time-consuming nature of model generation, and the lack of consensus on the approval and use of such technologies [15] may have hindered their clinical implementation [16].

More recently, the use of statistical models, based on femur shape and densitometric features, has emerged as a promising alternative approach with which to obtain information regarding fracture risk. Statistical models of femoral shape and intensity (i.e. density), based on Principal Component Analysis (PCA), were shown to improve the ability of aBMD to differentiate between fracture and non-fracture cases [17–19]. Aldieri et al. recently proposed a Partial Least Square (PLS)-based approach using QCT scans which achieved extremely good accuracy for hip fracture within a retrospective clinical cohort [20]. Being based on the maximisation of the covariance between shape or density and the risk of fracture, PLS was proved superior to PCA in separating fracture from non-fracture cases, as the most variable shape or intensity features might not be those most correlated with the risk of fracture [21].

Our hypothesis is that QCT-based models intrinsically show superior accuracy over aBMD when predicting fracture risk in patients with and without hip fractures, due to the increased quantity and quality of information they contain. However, QCT scans are not routinely performed during the diagnosis of osteoporosis and DXA remains the current clinical gold standard for the assessment of fracture risk.

Therefore, the aims of this study were to (i) develop statistical shape-intensity models based on DXA images and (ii) assess their accuracy for hip fracture prediction within a retrospective cohort. QCT images were also available for the same cohort and those had been previously used to build analogous QCT-based statistical models [20]. The hip fracture prediction accuracy of the newly developed DXA-based statistical models were here also compared with those based on the QCT scans acquired on the same cohort.

2. Materials and methods

The statistical model construction was based on a retrospective cohort of Caucasian women who were at least 5 years postmenopausal. The cohort comprised 50 subjetcs (cases) (55–89 years old) who had sustained a proximal femur fracture, and 50 case-matched (age, height and weight) controls who had not sustained a proximal femur fracture. Further information regarding the study cohort and design have been reported previously [22]. In order that the same case-control matched pairs used to build the QCT-based models presented in Aldieri et al. (2022) [20] were included when building the DXA-based statistical models, the DXA scans from a total of 88 participants (with hip fracture: $n = 43$, without hip fracture: $n = 45$) were used. The participant characteristics are reported in Table 1.

Table 1
Age, mass, height and neck aBMD, reported in terms of mean and standard deviation (SD), for the analysed cohort. Data for participants with (cases) and without hip fracture (controls) are shown separated.

	With hip fracture (cases) ($n = 43$)		Without hip fracture (controls) ($n = 45$)	
	Mean	SD	Mean	SD
Age	76	9	79	9
Mass (kg)	63.14	14.70	64.00	12.21
Height (m)	1.59	0.07	1.58	0.05
aBMD (g/cm^2)	0.59	0.12	0.63	0.10

In the following, the construction of the DXA-based two-dimensional statistical models will be detailed. As far as the construction of the CT-based models is concerned, which followed the same workflow here explained, we refer the reader to [20].

2.1. Processing of 2D femur shapes

Raw DXA images were imported and segmented in Matlab (R2023a, Mathowrks, Natick, Massachusetts, USA), where the 2D scan profiles were extracted as labelmaps at first, and later converted to polylines. These scan profiles were realigned so that (i) the centre of the most distal edge of the scan profile was set to be the origin and (ii) all the shaft axes were coincident. Eventually, the iterative closest point algorithm was employed to further improve the realignment. The realigned profiles (Fig. 1s in the Electronic Supplementary Material) were inputted into *Deformetrica* software [20,21,23]. *Deformetrica* outputted the mean anatomical shape and the moment vectors β^i, which are representative of the patient-specific shape features. More in detail, the moment vectors β^i, centred on a common grid of control points, define the deformations that the template should undergo in order to match each i^{th} participant-specific femur shape (Fig. 1). The generic i^{th} ($i = 1 \ldots N$, where N is the number of participants) subject-specific moment vectors can be expressed as follows:

$$\beta^i = \beta^i_{x\,1}, \beta^i_{y\,1}, \ldots, \beta^i_{x\,q}, \beta^i_{y\,q} \tag{1}$$

where i refers to the participant and q to the total number of moment vectors, defined in two dimensions (x,y). The (N x $2q$) shape matrix X_β (Fig. 1) was built by storing each β^i in the i^{th} row of the matrix. Further technical details about *Deformetrica* framework are contained in the Electronic Supplementary Material.

2.2. Statistical models

As two-dimensional shape and densitometric information was available from the DXA images, shape (SSM), intensity (SIM) and shape-intensity models (SSIM) were built. The statistical models were developed using a Partial Least Square (PLS)-based approach as described in [24]. This enabled the directions (also called modes) of maximal covariance between the shape, intensity or their combination and the known fracture status of the subjects to be determined [25], in accordance to Eq. (2):

$$x^i = \bar{x} + \sum_{j=1}^{m} t^i_j p_j \tag{2}$$

PLS identifies the modes, p_j, which define the bases of the new reference system where covariance is maximised. Hence, the original subject-specific generic features x^i can be represented in the new reference system defined by the modes as the components t^i_j, i.e., the projections of the original features onto each j^{th} mode.

The SSM was built by applying PLS to the N x $2q$ shape matrix X_β and to the fracture status array (Fig. 1, upper row). Similarly, the SIM was developed starting from the pixel-by-pixel aBMD map, described as follows. The template (i.e. the average shape obtained from *Deformetrica*) was meshed with triangular elements (0.5 mm edge length) using Hypermesh (2019, Altair Engineering Inc., Troy, USA). Subsequently, the template mesh was morphed using the previously obtained subject-specific moment vectors onto each subject's femur shape. In this way, isotopological meshes were obtained which enabled consistent sampling of the local aBMD from the participants' DXA images. Each mesh node was assigned with the aBMD value of the pixel it belonged, so that a N x n (with n the number of nodes) intensity matrix G was built gathering the participant-specific intensity vectors (i.e. the whole sets of the nodal density values, Fig. 1, lower row). The SIM was obtained by applying PLS onto the intensity matrix G and the fracture status array. The

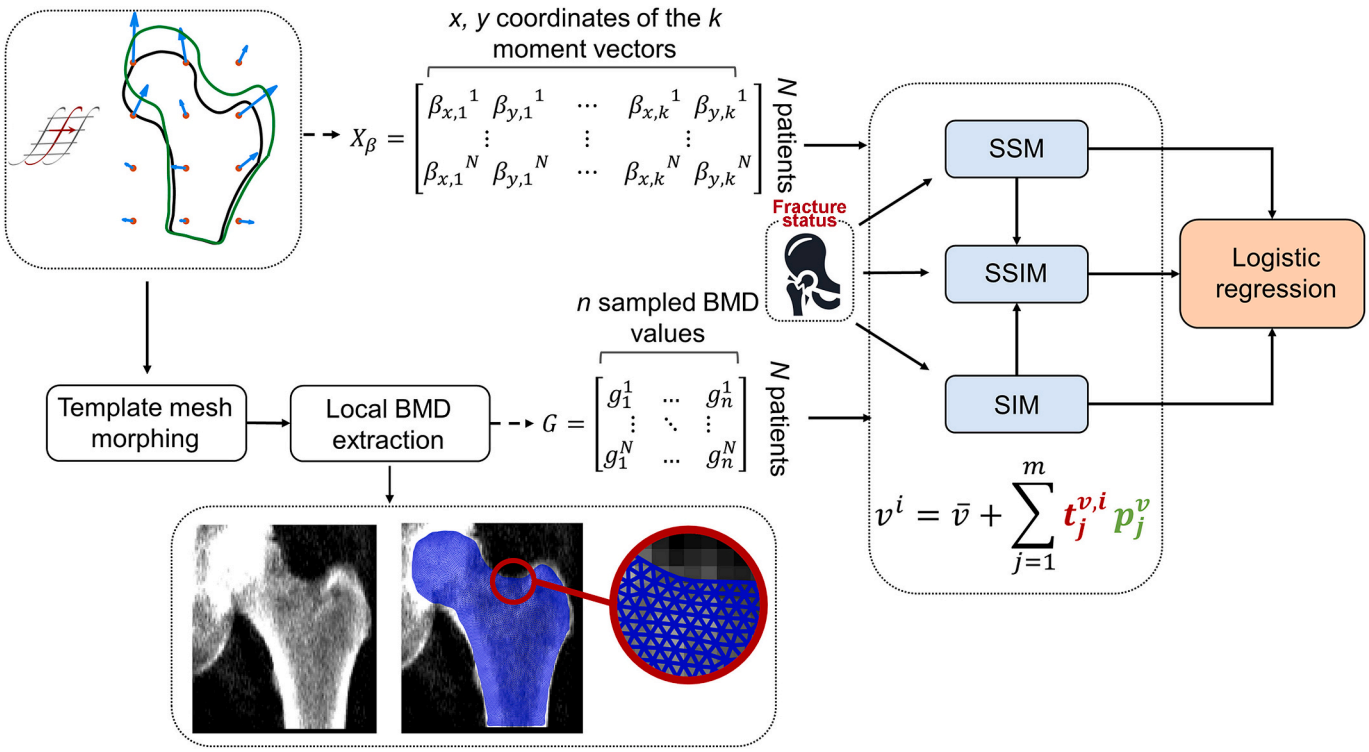

Fig. 1. Schematic representation of the workflow adopted to predict the hip fracture risk based on the statistical models built. The shape matrix X_β was built starting from the moment vectors output by *Deformetrica*. In the top left corner, the template is visible shown in black, with the moment vectors (light blue) guiding its transformation to the subject-specific shape, shown in green. The shape matrix X_β was then given as input to the PLS algorithm together with the known fracture status of the subjects, for the SSM construction. The moment vectors were also employed to morph the meshed template onto each DXA, so that the density matrix G was built and used with the fracture status array to build the SIM. In the lower part of the figure, a subject-specific DXA scan without and with the morphed meshed template (in blue) superimposed is presented. Eventually, the SSIM was obtained by combining the PLS components related to the SSM and the SIM. The reported equation refers to the generic variable v of the i^{th} subject, highlights the components ($t_j^{v,i}$, in red) and the modes (p_j^v, in green). The SSM, SIM and SSIM components ($t_j^{v,i}$) were used to train logistic regression models for the prediction of the fracture risk. (For interpretation of the references to colour in this figure legend, the reader is referred to the web version of this article.)

presence of outliers affecting the PLS-based methodology was assessed during the SSM and SIM construction by calculating the Cook's distance within a leave-one-out approach, as suggested in [26]. With the purpose of combining the independent SSM and SIM, a SSIM, intended to account for the combined shape and density distributions, was built [27]. Its construction relied on the shape and intensity PLS components, which were concatenated into a unique matrix to be used as a new PLS input. Further technical details about the statistical models construction can be found in [20,21].

2.3. Prediction of fracture risk

A logistic regression analysis was carried out between the PLS components, taken as independent predictors, and the fracture status, taken as the binary dependent variable. More specifically, the first three PLS components of the SSM, SIM and SSIM were considered here as independent predictors, leading to three distinct predictive models. The receiver operating characteristic (ROC) analyses of these logistic regression models were compared to that of the aBMD. The stratification accuracy of the developed statistical models was compared to that of the aBMD following a 10-fold cross-validation procedure [20], as the number of participants was too small to define separate training and test sets. PLS was performed and the logistic regression models were trained and tested 10 different times, predicting the fracture risk for the participants included in the test group. Each group consisted, as far as possible, of the same number of participants (i) with fracture and (ii) without fracture, to ensure an adequate balance within the training set. Area under the curve (AUC) was computed as a metric to determine the stratification performances of the different logistic regression models. The existence of statistically significant differences between the obtained AUC was also assessed, using DeLong test [28].

3. Results

A total of 7 shape modes were required to explain at least 90 % of the variance found in the shape, while all the shape modes taken together could only explain 33 % of the variability in the fracture risk. Fig. 2 shows the first 4 modes, which explained 76 % of the shape variability in the population. Interestingly, significant correlations ($p < 0.05$) could be found between the DXA- and CT-based modes, for the II and III DXA-based shape modes in particular. Further details about the identified correlations are provided in the Electronic Supplementary Material.

If the intensity modes are considered, 40 modes were required to describe 90 % of the intensity variability, while 7 modes could gather 90 % of the variability in the fracture risk. Fig. 3 shows the first 4 intensity modes, able alone to explain 77 % of the hip fracture risk variability. In this case, a significant correlation ($p < 0.001$) could be identified between the first mode and the first CT-based mode, as both describe a general increase/decrease in density across the femur as a whole (further details in the Electronic Supplementary Material).

As far as the SSIM is concerned, 32 modes were required to explain at least 90 % of the shape-intensity variability, while the first 4 modes, reported in Fig. 4, captured the same amount of variability in the fracture risk. Consistently with the previously obtained results, in this case significant correlation with the CT-based modes ($p < 0.001$) could be identified for the first three modes, as better detailed in the Electronic

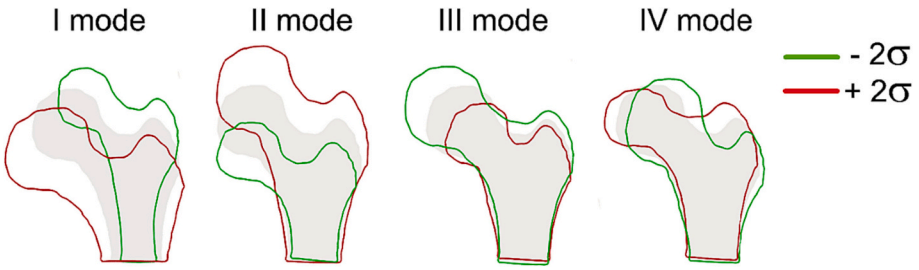

Fig. 2. The first four PLS shape modes, displayed as $\pm 2\sigma$ deformations of the template, shown in grey. σ refers to the specific mode standard deviation.

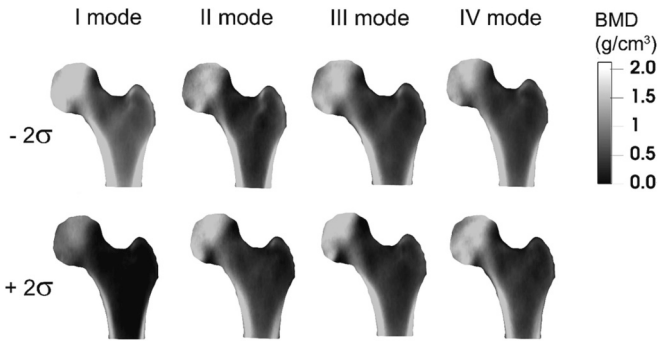

Fig. 3. The first four PLS intensity modes, displayed as $\pm 2\sigma$ variations along each mode. σ refers to the specific mode standard deviation.

Supplementary Material.

Fig. 5 displays the PLS components obtained for the SSM, SIM and SSIM respectively, depicted in different colours to differentiate the fractured from the non-fractured patients. As seen, when the aBMD information are included in the models, the separation between the two groups improves considerably.

Eventually, Fig. 6 presents the comparison of the different ROC curves obtained from the 10-fold cross validation: significant differences ($p < 0.05$) between the SSM AUC and the SIM and SSIM AUCs emerged, but the SIM and SSIM AUC did not result to be significantly different. In addition, the SSIM AUC turned out to be significantly higher than the T-score related AUC.

4. Discussion

The aim of this study was to assess whether the current prediction of the hip fracture risk based on the aBMD-derived T-score could be improved by considering the local aBMD information contained in a DXA image as a whole, i.e. by considering the proximal femur geometry and the entire pixel-by-pixel aBMD set of values contained in a DXA scan. In order to do this, a SSM, a SIM and a SSIM based on PLS algorithm were built starting with the DXA images of 88 participants with known hip fracture status. Logistic regression models were developed using the shape, intensity, and shape-intensity PLS components to predict the fracture risk. The outcomes of these models in terms of classification accuracy were then compared to the aBMD based on a 10-fold cross validation procedure.

Density was able to explain most of the variability in the hip fracture and in fact the AUC corresponding to the SIM was significantly higher compared to the SSM-related AUC, in agreement with [29,30]. However, the SSIM, combining shape and density combined managed to slightly outperform the SIM, and statistically significant differences were identified between the SSIM and aBMD AUC values. Hence, the proximal femur shape and local density features contained in the DXA scans were shown to enhance hip fracture risk assessment. Overall, density was confirmed to play a key role in determining the risk of fracture: despite exhibiting very variable features across the population, as witnessed by the number of modes required to explain 90 % of the total variance, few modes were sufficient to explain >90 % of the variance in the fracture risk. Shape and densitometric properties, deterministically affecting osteoporosis-related hip fracture risk prediction, have been examined during this study. However, other factors, not considered here, may also play an important role. In fact, osteoporosis-related hip fractures represent complex events, mostly caused by falls, which cannot be treated deterministically. QCT-derived digital twins can take these aspects into account and have been successfully proven to improve fracture risk prediction [6,7,15,31,32]. Nevertheless, as these are based on QCT images, patient-specific models cannot currently be included in the standard clinical care. Grassi et al. have recently presented a work where the possibility to develop three-dimensional patient-specific models from DXA images was demonstrated and shown to outperform aBMD predictions [33]. Although

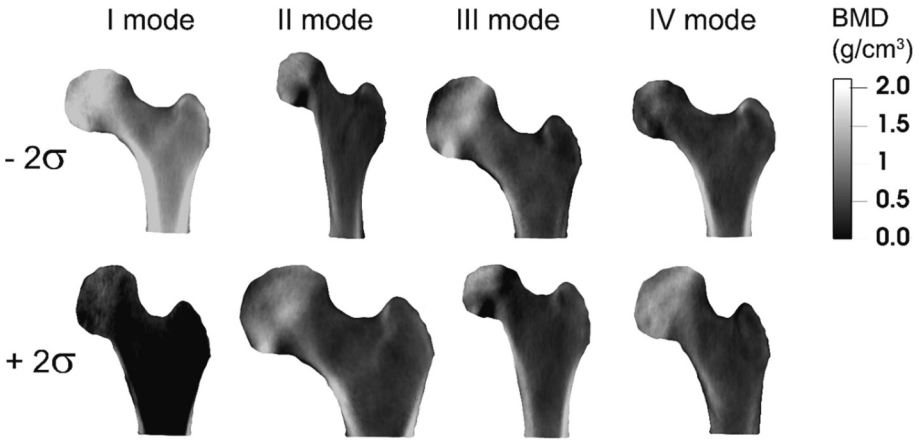

Fig. 4. The first four PLS shape-intensity modes, displayed as $\pm 2\sigma$ variations along each mode. σ refers to the specific mode standard deviation.

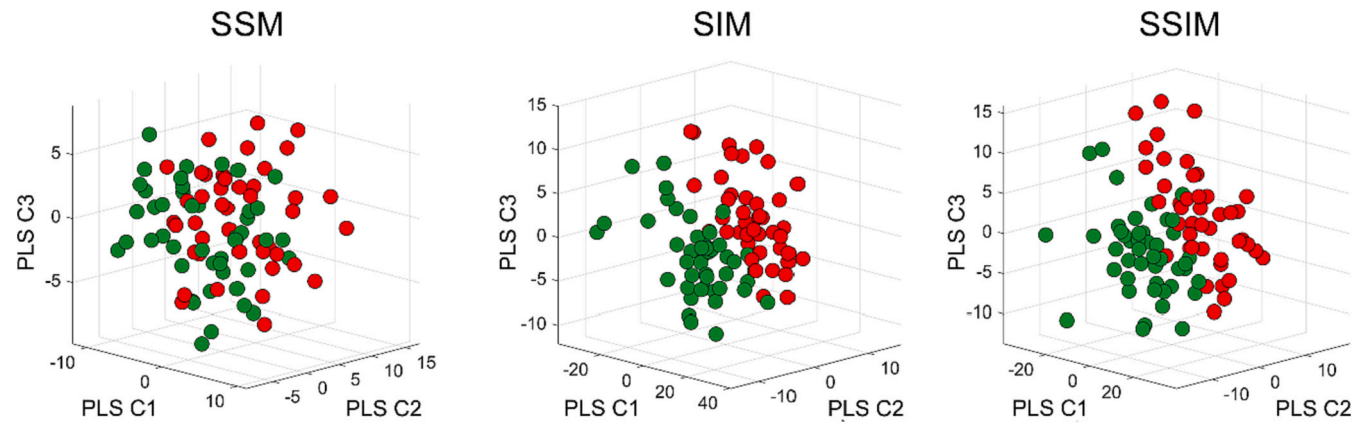

Fig. 5. First three shape, intensity and shape-intensity PLS components. The components of the participants with fracture and the participants without fracture are show in red and green, respectively. (For interpretation of the references to colour in this figure legend, the reader is referred to the web version of this article.)

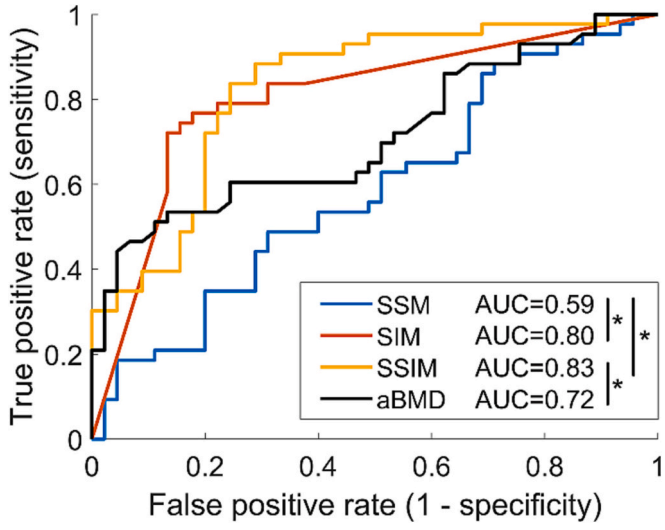

Fig. 6. ROC curves resulting from the 10-fold cross-validation. ROC curves resulting from the logistic regression models implemented are compared with the aBMD ROC curve. AUC values turned out to be 0.59 (95 % CI 0.47–0.69), 0.80 (95 % CI 0.70–0.90), 0.83 (95 % CI 0.73–0.90) and 0.72 (95 % CI 0.59–0.82) for the SSM, SIM, SSIM and aBMD-based predictive models.

working on a prospective cohort much larger than that presented here, they obtained AUC values for the aBMD comparable to those here reported. Instead, as expected, the AUC achieved by the three-dimensional FE model predictions turned out to be superior to those yielded here by the best PLS components-based logistic model. Three-dimensional FE models can in fact consider the fracture event as a whole and could thus take into account its complexity. Despite being integrated with additional derived information to derive the three-dimensional models, also in [33] the only patient-specific original data was represented by DXA. Therefore, DXA appeared to contain per se valuable information beyond the average aBMD employed in clinical practice. From this perspective, the here presented study strictly focused on DXA information and tried to exploit it fully, achieving promising results. The fracture risk prediction, although less accurate than in [33], was implemented in a simpler way and with low computational cost. Although the training phase requires some time, especially due to the need of running sensitivity analyses on *Deformetrica* input parameters, once the PLS space and the logistic regression models are defined, the components of any new subjects could be identified by projection on the PLS space and finally the subject-specific fracture risk established by means of the logistic regression models within minutes. Contrary to [33], in this study a retrospective cohort was employed, where DXA was acquired after the fracture event and on the contralateral femur, which might seem to bring some limitations. However, because the fracture event occurred no earlier than 90 days prior to the DXA scan, considerable changes in shape and densitometric features were not expected to have occurred [22,34]. Similarly, since none of the patients suffered from pathologies such as bone tumours or dysplasia, neglectable differences between the two femur bones were expected. In this light, the use of a prospective cohort would not be judged to affect dramatically the achieved outcomes. On the whole, the possibility to exploit DXA fully, improving T-score predictions, confirmed there could be room for improvement in the clinical diagnostic path currently in place. On top of that, the identified correlation between the DXA- and CT-based modes corroborated the hypothesis the pixel-by-pixel aBMD values available in DXA images are worth being considered. In summary, the here proposed methodology proved to be promising, particularly due to the possibility of being included in the current diagnostic pipeline without adding complexity to it. The ambition of this study was not to propose a fully implemented methodology, rather to preliminarily assess its potential.

Larger prospective cohorts would be needed to identify PLS modes more robustly and to properly test the accuracy of the proposed methodology on a separate dedicated test set. Once identified, the PLS modes might be employed to extract the components for any new subject and eventually to carry out the fracture prediction.

Fundings

This research did not receive any specific grant from funding agencies in the public, commercial, or not-for-profit sectors.

CRediT authorship contribution statement

Alessandra Aldieri: Writing – review & editing, Writing – original draft, Methodology, Formal analysis, Conceptualization. **Margaret Paggiosi:** Writing – review & editing, Methodology, Data curation. **Richard Eastell:** Writing – review & editing, Conceptualization. **Cristina Bignardi:** Writing – review & editing, Methodology, Conceptualization. **Alberto L. Audenino:** Writing – review & editing, Methodology, Conceptualization. **Pinaki Bhattacharya:** Writing – review & editing, Supervision, Methodology, Conceptualization. **Mara Terzini:** Writing – review & editing, Supervision, Methodology, Conceptualization.

Declaration of competing interest

The authors declare that they have no known competing financial interests or personal relationships that could have appeared to influence the work reported in this paper.

Data availability

Data will be made available on request.

References

[1] E. Hernlund, et al., Osteoporosis in the European Union: medical management, epidemiology and economic burden. A report prepared in collaboration with the international osteoporosis foundation (IOF) and the European Federation of Pharmaceutical Industry Associations (EFPIA), Arch. Osteoporos. 8 (1) (2013) 136, https://doi.org/10.1007/s11657-013-0136-1.

[2] J.A. Kanis, E.V. McCloskey, H. Johansson, A. Oden, L.J. Melton, N. Khaltaev, A reference standard for the description of osteoporosis, Bone 42 (3) (2008) 467–475, https://doi.org/10.1016/j.bone.2007.11.001.

[3] S.C.E. Schuit, et al., Fracture incidence and association with bone mineral density in elderly men and women: the Rotterdam study, Bone 34 (1) (2004) 195–202, https://doi.org/10.1016/j.bone.2003.10.001.

[4] K.L. Stone, et al., BMD at multiple sites and risk of fracture of multiple types: long-term results from the study of osteoporotic fractures, J. Bone Miner. Res. 18 (11) (2003) 1947–1954, https://doi.org/10.1359/jbmr.2003.18.11.1947.

[5] J.A. Kanis, et al., The need to distinguish intervention thresholds and diagnostic thresholds in the management of osteoporosis, Osteoporos. Int. 34 (1) (2023) 1–9, https://doi.org/10.1007/s00198-022-06567-9.

[6] A. Aldieri, et al., Personalised 3D assessment of trochanteric soft tissues improves HIP fracture classification accuracy, Ann. Biomed. Eng. 50 (3) (2022) 303–313, https://doi.org/10.1007/s10439-022-02924-1.

[7] I. Fleps, et al., Finite element derived femoral strength is a better predictor of hip fracture risk than aBMD in the AGES Reykjavik study cohort, Bone 154 (2022) 116219, https://doi.org/10.1016/j.bone.2021.116219.

[8] D.L. Kopperdahl, et al., Assessment of incident spine and hip fractures in women and men using finite element analysis of CT scans, J. Bone Miner. Res. 29 (3) (2014) 570–580, https://doi.org/10.1002/jbmr.2069.

[9] E.S. Orwoll, et al., Finite element analysis of the proximal femur and hip fracture risk in older men, J. Bone Miner. Res. 24 (3) (2009) 475–483, https://doi.org/10.1359/jbmr.081201.

[10] M. Qasim, et al., Patient-specific finite element estimated femur strength as a predictor of the risk of hip fracture: the effect of methodological determinants, Osteoporos. Int. 27 (9) (2016) 2815–2822, https://doi.org/10.1007/s00198-016-3597-4.

[11] A.L. Adams, et al., Osteoporosis and hip fracture risk from routine computed tomography scans: the fracture, osteoporosis, and CT utilization study (FOCUS), J. Bone Miner. Res. 33 (7) (2018) 1291–1301, https://doi.org/10.1002/jbmr.3423.

[12] A. Aldieri, C. Curreli, J.A. Szyszko, A.A. La Mattina, M. Viceconti, Credibility assessment of computational models according to ASME V&V40: application to the Bologna biomechanical computed tomography solution, Comput. Methods Programs Biomed. 240 (2023) 107727, https://doi.org/10.1016/j.cmpb.2023.107727.

[13] A. Aldieri, et al., Osteoporotic hip fracture prediction: is T-score-based criterion enough? A hip structural analysis-based model, J. Biomech. Eng. 140 (111004) (2018), https://doi.org/10.1115/1.4040586.

[14] C.R. Shuhart, et al., Executive summary of the 2019 ISCD position development conference on monitoring treatment, DXA cross-calibration and least significant change, spinal cord injury, Peri-prosthetic and orthopedic bone health, transgender medicine, and pediatrics, J. Clin. Densitom. 22 (4) (2019) 453–471, https://doi.org/10.1016/j.jocd.2019.07.001.

[15] I. Fleps, E.F. Morgan, A review of CT-based fracture risk assessment with finite element modeling and machine learning, Curr. Osteoporos. Rep. 20 (5) (2022) 309–319, https://doi.org/10.1007/s11914-022-00743-w.

[16] M. Terzini, A. Aldieri, L. Rinaudo, G. Osella, A.L. Audenino, C. Bignardi, Improving the hip fracture risk prediction through 2D finite element models from DXA images: validation against 3D models, Frontiers in Bioengineering and Biotechnology 7 (2019). Accessed: Feb. 12, 2024. [Online]. Available: https://www.frontiersin.org/articles/10.3389/fbioe.2019.00220.

[17] J.C. Baker-LePain, K.R. Luker, J.A. Lynch, N. Parimi, M.C. Nevitt, N.E. Lane, Active shape modeling of the hip in the prediction of incident hip fracture, J. Bone Miner. Res. 26 (3) (2011) 468–474, https://doi.org/10.1002/jbmr.254.

[18] S.R. Goodyear, et al., Can we improve the prediction of hip fracture by assessing bone structure using shape and appearance modelling? Bone 53 (1) (2013) 188–193, https://doi.org/10.1016/j.bone.2012.11.042.

[19] G. Pascoletti, A. Aldieri, M. Terzini, P. Bhattacharya, M. Calì, E.M. Zanetti, Stochastic PCA-based bone models from inverse transform sampling: proof of concept for mandibles and proximal femurs, Appl. Sci. 11 (11) (2021), https://doi.org/10.3390/app11115204. Art. no. 11, Jan.

[20] A. Aldieri, et al., Improving the hip fracture risk prediction with a statistical shape-and-intensity model of the proximal femur, Ann. Biomed. Eng. 50 (2) (2022) 211–221, https://doi.org/10.1007/s10439-022-02918-z.

[21] A. Aldieri, M. Terzini, A.L. Audenino, C. Bignardi, U. Morbiducci, Combining shape and intensity dxa-based statistical approaches for osteoporotic HIP fracture risk assessment, Comput. Biol. Med. 127 (2020) 104093, https://doi.org/10.1016/j.compbiomed.2020.104093.

[22] L. Yang, W.J.M. Udall, E.V. McCloskey, R. Eastell, Distribution of bone density and cortical thickness in the proximal femur and their association with hip fracture in postmenopausal women: a quantitative computed tomography study, Osteoporos. Int. 25 (1) (2014) 251–263, https://doi.org/10.1007/s00198-013-2401-y.

[23] S. Durrleman, et al., Morphometry of anatomical shape complexes with dense deformations and sparse parameters, NeuroImage 101 (2014) 35–49, https://doi.org/10.1016/j.neuroimage.2014.06.043.

[24] R. Rosipal, N. Krämer, Overview and recent advances in partial least squares, in: C. Saunders, M. Grobelnik, S. Gunn, J. Shawe-Taylor (Eds.), Subspace, Latent Structure and Feature Selection, Springer, Berlin, Heidelberg, 2006, pp. 34–51, https://doi.org/10.1007/11752790_2. Lecture Notes in Computer Science.

[25] M. Barker, W. Rayens, Partial least squares for discrimination, J. Chemometr. 17 (3) (2003) 166–173, https://doi.org/10.1002/cem.785.

[26] J.L. Bruse, et al., A statistical shape modelling framework to extract 3D shape biomarkers from medical imaging data: assessing arch morphology of repaired coarctation of the aorta, BMC Med. Imaging 16 (1) (2016) 40, https://doi.org/10.1186/s12880-016-0142-z.

[27] M. B. Stegmann and R. Fisker, 'Active Appearance Models: Theory and Cases'.

[28] E.R. DeLong, D.M. DeLong, D.L. Clarke-Pearson, Comparing the areas under two or more correlated receiver operating characteristic curves: a nonparametric approach, Biometrics 44 (3) (1988) 837–845.

[29] J.S. Gregory, D. Testi, A. Stewart, P.E. Undrill, D.M. Reid, R.M. Aspden, A method for assessment of the shape of the proximal femur and its relationship to osteoporotic hip fracture, Osteoporos. Int. 15 (1) (2004) 5–11, https://doi.org/10.1007/s00198-003-1451-y.

[30] J.S. Gregory, R.M. Aspden, Femoral geometry as a risk factor for osteoporotic hip fracture in men and women, Med. Eng. Phys. 30 (10) (2008) 1275–1286, https://doi.org/10.1016/j.medengphy.2008.09.002.

[31] P. Bhattacharya, Z. Altai, M. Qasim, M. Viceconti, A multiscale model to predict current absolute risk of femoral fracture in a postmenopausal population, Biomech. Model. Mechanobiol. 18 (2) (2019) 301–318, https://doi.org/10.1007/s10237-018-1081-0.

[32] E. Schileo, F. Taddei, Finite element assessment of bone fragility from clinical images, Curr. Osteoporos. Rep. 19 (6) (2021) 688–698, https://doi.org/10.1007/s11914-021-00714-7.

[33] L. Grassi, et al., 3D finite element models reconstructed from 2D dual-energy X-ray absorptiometry (DXA) images improve hip fracture prediction compared to areal BMD in osteoporotic fractures in men (MrOS) Sweden cohort, J. Bone Miner. Res. 38 (9) (2023) 1258–1267, https://doi.org/10.1002/jbmr.4878.

[34] H. Burger, et al., The association between age and bone mineral density in men and women aged 55 years and over: the Rotterdam study, Bone Miner. 25 (1) (1994) 1–13, https://doi.org/10.1016/S0169-6009(08)80203-6.